HHS Public Access

Author manuscript

Xenobiotica. Author manuscript; available in PMC 2016 June 08.

Published in final edited form as:

Xenobiotica. 2015 ; 45(11): 990–998. doi:10.3109/00498254.2015.1038743.

IN VITRO GLUCURONIDATION OF APREPITANT: A MODERATE INHIBITOR OF UGT2B7

Larry House, **Jacqueline Ramirez**, **Michael Seminerio**, **Snezana Mirkov**, and **Mark J. Ratain**

Department of Medicine, University of Chicago, Chicago, IL, USA

Abstract

1. Aprepitant, an oral antiemetic, commonly used in the prevention of chemotherapy-induced nausea and vomiting, is primarily metabolized by CYP3A4. Aprepitant glucuronidation has yet to be evaluated in humans. The contribution of human UDP-glucuronosyltransferase (UGT) isoforms to the metabolism of aprepitant was investigated by performing kinetic studies, inhibition studies, and correlation analyses. In addition, aprepitant was evaluated as an inhibitor of UGTs.

2. Glucuronidation of aprepitant was catalyzed by UGT1A4 (82%), UGT1A3 (12%), and UGT1A8 (6%) and K_ms were 161.6 ± 15.6 μM, 69.4 ± 1.9 μM, and 197.1 ± 28.2 μM, respectively. Aprepitant glucuronidation was significantly correlated with both UGT1A4 substrates anastrazole and imipramine (r_s = 0.77, P < 0.0001 for both substrates; n = 44), and with the UGT1A3 substrate thyroxine (r_s = 0.58, P < 0.0001; n = 44).

3. We found aprepitant to be a moderate inhibitor of UGT2B7 with a K_i of ~10 μM for 4-MU, morphine, and zidovudine. Our results suggest aprepitant can alter clearance of drugs primarily eliminated by UGT2B7. Given the likelihood for first-pass metabolism by intestinal UGT2B7, this is of particular concern for oral aprepitant co-administered with oral substrates of UGT2B7, such as zidovudine and morphine.

Keywords

Aprepitant; drug metabolism; phase II

Introduction

Aprepitant is an orally administered neurokinin receptor antagonist commonly used in the prevention of chemotherapy-induced nausea and vomiting (Olver, 2004). Phase I metabolism studies have suggested aprepitant is both a substrate and a moderate inhibitor of CYP3A4 (Sanchez et al., 2004) as well as a moderate inducer of CYP2C9 (Shadle et al., 2004). The number of phase II metabolism studies have been less extensive. One study has found that glucuronidation is a significant route for elimination of aprepitant in rats and dogs and further suggested that enterohepatic recycling of the parent drug may occur since

Address for correspondence: Dr. Mark J. Ratain, Department of Medicine, University of Chicago, 5841 S. Maryland Ave., MC2115, Chicago, IL 60637, USA. mratain@medicine.bsd.uchicago.edu.

aprepitant glucuronide was abundantly detected in rat bile but absent in feces (Huskey et al., 2003).

UDP-glucuronosyltransferases (UGTs) are known to play a significant role in the metabolism of xenobiotics, as well as endogenous compounds (Kaivosaari et al., 2011). The UGT family catalyzes glucuronidation of lipophilic compounds with the formation of a β-D-glucuronide product (more water-soluble and therefore easier to be excreted) (King et al., 2000). The precise role of UGTs in the metabolism of aprepitant has not yet been studied in humans. Moreover, the overall impact of aprepitant glucuronidation has yet to be evaluated for potential drug interactions. Therefore, in the study presented herein, we aim to elucidate the major UGT isoforms involved in the glucuronidation of aprepitant *in vitro*, and evaluate aprepitant as a potential UGT inhibitor.

Materials and Methods

Chemicals and Reagents

Aprepitant, aprepitant-13C2,d2, aprepitant-β-glucuronide, 3'-azido-3'-deoxythymidine (AZT), and AZT-3-β-D-glucuronide (AZT-G) were purchased from Toronto Research Chemicals, Inc. (North York, ON, CA). Morphine, morphine-6-β-D-glucuronide (M-6-G), 10,11-dihydrocarbamazapine, 4-methylumbelliferone (4-MU), triamcinolone, and 4-methylumbelliferyl-β-D-glucuronide hydrate (4-MU-G) were purchased from Sigma-Aldrich (St. Louis, MO). Uridine 5'-diphospho-glucuronic acid (UDPGA) (UGT Rxn mix Solution A), 250 mM Tris-HCl (pH 7.5) buffer mix with 40 mM $MgCl_2$ and 0.125 mg/ml alamethicin (UGT Rxn mix Solution B), UGT1A1, UGT1A3, UGT1A4, UGT1A6, UGT1A7, UGT1A8, UGT1A9, UGT1A10, UGT2B4, UGT2B7, UGT2B10, UGT2B15, UGT2B17, UGT control Supersomes, and human intestinal microsomes (HIM) were purchased from BD Biosciences (Woburn, MA). Human liver microsomes (HLM) were processed through Dr. Mary Relling's laboratory at St. Jude Children's Research Hospital (Memphis, TN). Livers were obtained through the Liver Tissue Cell Distribution System (funded by #NO1-DK-9-2310) and the Cooperative Human Tissue Network. Protein concentrations were measured using the Qubit® protein assay kit (Invitrogen Life Technologies, Grand Island, NY).

General UGT Assay Incubation Conditions for Aprepitant Glucuronidation

General UGT assay conditions were adopted from (Walsky et al., 2012) with minor modifications. Briefly, aprepitant was pre-incubated with pooled HLMs, UGTs, or HIMs (0.5 mg of protein/ml) at 37°C for 5 minutes in a buffer mix (UGT Rxn mix Solution B) containing Tris-HCl (pH 7.5), $MgCl_2$, and alamethicin (final concentrations of 50 mM, 8 mM, and 25 μg/ml respectively). After pre-incubation for 5 minutes, the reaction was started with the addition of UDPGA (UGT Rxn mix Solution A) (2 mM final concentration). The total reaction volume was 100 μl. Aprepitant was dissolved in 100% DMSO. Final organic solvent concentrations were 1% (v/v). After incubation at 37°C for 60 minutes, incubation samples were terminated by combining with an equal volume of internal standard (1 μM triamcinolone in methanol), vortexed and centrifuged at 20,817 RCF for 15 minutes (4°C). The supernatant was transferred to a polypropylene HPLC vial and 10 μl was injected into

the LC-MS/MS for analysis. All samples were performed in triplicate and data are represented as means ± S.D. [%CV] unless otherwise noted.

Optimization of Assay Incubation Conditions and K_m Determination in HLMs, HIMs and relevant UGTs

Linearity of product formation with respect to time (2.5–90 min) and protein concentration (0.1–1 mg/ml) were conducted for aprepitant glucuronidation in HLMs and HIMs only. After optimization for time and protein concentration (utilizing a substrate concentration of 250 μM), we used ten aprepitant concentrations ranging from 5 μM to 250 μM for the determination of K_m in HLMs, HIMs, and relevant UGTs (UGT1A3, UGT1A4 and UGT1A8).

Screening for Aprepitant Glucuronidation

We measured aprepitant glucuronidation utilizing HLMs, HIMs, recombinant UGT1A1, UGT1A3, UGT1A4, UGT1A6, UGT1A7, UGT1A8, UGT1A9, UGT1A10, UGT2B4, UGT2B7, UGT2B15, UGT2B10, UGT2B17, and UGT control. Substrate concentrations of 5 and 250 μM were used. All samples were incubated under conditions as described above.

Inhibition of Aprepitant Glucuronidation

HLMs and HIMs were incubated at clinically relevant aprepitant (substrate) concentrations of 5 μM (Lasseter et al., 2007; Takahashi et al., 2011). UGT1A3, UGT1A4, and UGT1A8 were incubated at the respective K_ms for aprepitant of 69 μM, 162 μM, and 197 μM. Inhibitor concentrations for UGT1A3 (sulfinpyrazone 1000 μM), UGT1A4 (hecogenin 200 μM) (Uchaipichat et al., 2006), and UGT1A8 (diclofenac 500 μM) (Uchaipichat et al., 2004) were used for each respective Supersome. Negative controls were performed in the absence of inhibitors. All incubation conditions were performed as described above.

HLM Correlation Analysis

A panel of HLMs from 44 individual donors was incubated with 30 μM aprepitant and assayed for aprepitant glucuronide (AP-G) activity. The incubation conditions are described above. We correlated this data with our previously published experimental data for thyroxine-G (UGT1A3 substrate) (Yoder Graber et al., 2007), anastrazole-G (UGT1A4 substrate) (Kamdem et al., 2010), and imipramine-G (UGT1A4 substrate) (Kamdem et al., 2010).

LC-MS/MS Assay of AP-G

A sensitive LC-MS/MS assay was modified from a previously published method to identify and quantify AP-G (Wu et al., 2009). After incubations were performed as described above, AP-G and the internal standard (triamcinolone, 1.0 μM in methanol) were introduced onto an LC-MS/MS that consisted of an Agilent 1100 series pump and autosampler (Agilent, Santa Clara, CA) and an API 2000 LC-MS/MS triple quadruple system (Applied Biosystems, Foster City, CA). Aprepitant, AP-G, and the internal standard were separated on a 50 × 2.1 mm Luna 3 μm C_8 stainless steel column with a guard column of similar packing material (Phenomenex, Torrance, CA). The components were eluted with a gradient

consisting of 0.5% formic acid in water (pump 'A') and acetonitrile (pump 'B') delivered at a flow rate of 0.3 ml/min. A gradient was applied as follows: (0–1.6 min, 90% A), (1.6–2.5 min, switch from 90% A to 2% A), (2.5–4.2 min, 2% A), (4.3–10 min, 90% A). We utilized a valco valve to shunt away unnecessary components into a waste bottle. The LC eluate was introduced into an electrospray ionization (ESI) source at the same flow rate. The ESI voltage was set at +5000 V and a temperature of 550°C. The positive ion multiple reaction monitoring (MRM) mode analysis was performed using nitrogen as the collision gas. The curtain, collision, nebulizing, and heater gases were set at 35, 5, 50, and 70 psi respectively. For triamcinolone; declustering potential (DP), focusing potential (FP), entrance potential (EP), collision cell entrance potential (CEP), collision energy (CE), and collision cell exit potential (CXP) were 20, 400, 7, 20, 21, and 18 volts respectively. For aprepitant, AP-G, and aprepitant-13C2,d2; DP, FP, EP, CEP, CE, and CXP voltages were 30, 400, 8, 31, 40, and 9 volts respectively. A dwell time of 200 ms and a pause time of 5 ms between scans were used to monitor the precursor/product ion pairs. Since AP-G was not initially available at the time of our experiments, we tuned for AP-G by utilizing the optimized LC-MS/MS parameters for aprepitant, while substituting the known precursor ion mass (MH^+) of 711.2 amu for the glucuronide of aprepitant. We then tuned the instrument for two product ion masses (179.2 and 277 amu) and found the best signal to noise ratio for the MRM pair. The MRM transition pairs for aprepitant, AP-G, triamcinolone and aprepitant-13C2,d2 were (*m/z* 535.2/179.2), (*m/z* 711.2/179.2), (*m/z* 395.3/357.2), and (*m/z* 539.2/179.2) respectively. The retention times were 6.5 min for aprepitant, 6.1 min for AP-G, 5.6 min for triamcinolone, and 6.5 min for aprepitant-13C2,d2. The mass for AP-G was previously investigated and confirmed by our experimental data (Huskey et al., 2004). We prepared standards of aprepitant-13C2,d2 (for quantifying AP-G) in 50 mM Tris-HCl buffer (pH 7.5), aliquoted, stored at −80°C, and validated over three days (N=9) with a concentration range of 928 pM – 186 nM. Once AP-G became commercially available, we prepared and validated standards of the same concentration range and observed similar linear regression slopes for AP13C2,d2 and AP-G. Moreover, we repeated random points from our previous experiments with the authentic AP-G standards and confirmed similar results (data not shown).

Inhibition by Aprepitant of UGTs

In all inhibition experiments, aprepitant was added at 1 and 10 μM concentrations. 4-MU was used as the substrate for the measurement of inhibition of UGT1A1, UGT1A3, UGT1A6, UGT1A7, UGT1A8, UGT1A9, UGT1A10, UGT2B4, UGT2B7, UGT2B15, and UGT2B17 by aprepitant. Incubations contained 4-MU (concentrations specified in Dong et al., 2012), UGTs (protein concentrations found in Liu et al., 2010), 2.5 mM UDPGA, 8 mM $MgCl_2$, 25 μg/ml alamethicin, aprepitant (1 and 10 μM) and 50 mM Tris-HCl (pH 7.5). Positive controls for inhibition included 500 μM diclofenac for UGT1A1, UGT1A6, UGT1A7, UGT1A8, UGT1A9, UGT1A10, UGT2B7, UGT2B15 and UGT2B17; 1 mM sulfinpyrazone for UGT1A3; and 500 μM androsterone for UGT2B4. Reaction times have been previously described (Dong et al., 2012). Incubations were stopped, processed, and analyzed by HPLC as previously reported (Liu et al., 2010). Imipramine was used as UGT1A4 substrate. Incubations were performed as previously described (Nakajima et al., 2002). Hecogenin (200 μM in MeOH) was used as positive control for inhibition. Reactions

(100 μl) were stopped after 60 min with 100 μl of ice-cold acetonitrile and centrifuged at 20,817 RCF for 15 min (4°C). Aliquots (5 μl) were analyzed by HPLC. Elution was done with 28/72 acetonitrile/10 mM potassium phosphate monobasic (pH 2.6) (1 ml/min), an XTerra RP18 column (4.6 × 100 mm, 5 μm; Waters Corporation, Wood Dale, IL), a Nova-Pak C18 (4 μM) guard column (Waters Corporation, Wood Dale, IL) and UV detection (254 nm). Results are reported as percentages of inhibition of control activities determined in the absence of inhibitor. These experiments were performed in duplicate.

K_i Determination of Aprepitant on 4-MU-G, M-6-G, and AZT-G Formation in UGT2B7

A range of inhibitor concentrations for aprepitant of (0, 1, 2, 5, 10 and 20 μM) and substrate concentrations for 4-MU (168, 335, 670 μM) (Uchaipichat et al., 2004), morphine (325, 650, and 1300 μM) (Court et al., 2003), and AZT (385, 770, and 1540 μM) (Court et al., 2003) were incubated with similar conditions (as noted under *Inhibition by Aprepitant of UGTs*) with incubation times of 120, 30 and 240 minutes for 4-MU, morphine and AZT respectively and final UDPGA concentrations of 2.5, 5 and 5 mM for 4-MU, morphine and AZT respectively.

HPLC Assay Conditions for 4-MU-G, M-6-G, and AZT-G

Assay conditions for 4-MU can be found under *Inhibition by Aprepitant of UGTs*. Analytical conditions for M-6-G were based on a method previously used in this laboratory (Innocenti et al., 2001). For AZT-G analyses, we used a previously published method (Court et al., 2003) with slight modification. Briefly, incubations were terminated with addition of 100 μl ACN (with 1 mM p-acetomidophenol), vortexed and centrifuged at 20,817 RCF at 4°C for 30 min. The supernatant was transferred to a polypropylene HPLC vial and 10 μl was injected into the HPLC system. Separations were performed with a reversed phase μBondapak C_{18} column (10μm, 3.9 × 300 mm, Waters Corp.) preceded by a Novapak C_{18} guardpak (Waters Corp.) The mobile phase was a mixture of 20 mM, pH 2.2, potassium phosphate buffer in water (pump ‘A’), and acetonitrile with 5% water (pump ‘B’) at a flow rate of 1.0 ml/min. A gradient was applied as follows: 0 – 4.0 min, 80% A. 4.1 – 8.0 min, 50% A. 8.1 – 12.0 min, 30% A. 12.1 – 20 min 80% A. The respective retention times for AZT-G and the internal standard were 5.5 min and 7.3 min respectively.

K_i Determination of Aprepitant on M-6-G Formation in UGT2B7 with pHs of 6.5 and 7.5

A range of inhibitor concentrations for aprepitant of (0, 1, 2, 5, 10 and 20 μM) and a substrate concentration for morphine of 650 μM was incubated with similar conditions as noted above except two 400 mM Tris-HCl buffers were made (pH 6.5 and pH 7.5) to reflect a typical pH range in the human small bowel (Fallingborg, 1999).

Enzyme Kinetic Data Analysis

The kinetic parameters for aprepitant glucuronidation were calculated by fitting the untransformed experimental data to the following enzyme kinetic equations using Prism 5.2 (Graphpad software Inc., San Diego, CA), designed for nonlinear regression analysis. The selection of the “best-fit” kinetic model was based on the comparison of the sum-of-squared residuals, coefficient of determination (r^2), and shape of the Eadie-Hofstee plot (Prism 5.2).

The Michaelis-Menten equation was used when the Eadie-Hofstee plot exhibited a linear shape (Uchaipichat et al., 2004). The two enzyme Michaelis-Menten equation was used when the Eadie-Hofstee plot exhibited a biphasic shape (Court et al., 2003; Uchaipichat et al., 2004). The Hill equation was used when the Eadie-Hofstee plot exhibited a sigmoidal shaped curve (Hutzler et al., 2002; Uchaipichat et al., 2004).

$$[\mathrm{I}]=\mathrm{I}_{\mathrm{GUT}}=\mathrm{Molar}\ \ \mathrm{dose}/250\mathrm{mL} \quad (1)$$

The concentration of drug [I] in the lumen of the gut was calculated as (eq. 1) (Huang 2012; Zhang et al., 2008). The inhibition type was identified by plotting (1/V) against the inhibitor concentrations (1/[S]) (Chang et al., 2005).

Apparent K_i values for inhibition of 4-MU and AZT glucuronidation by aprepitant were determined by plotting (1/V) vs. [S], and where the (1/V) vs. [S] lines converged. Apparent K_i values for inhibition of morphine glucuronidation by aprepitant were determined by where the (1/V) vs. [S] line(s) intersected the abscissa 1/V = 0 (Chang et al., 2005).

Correlation Analysis

Correlational analyses between AP-G formation and the UGT activities of thyroxine-G, anastrazole-G, and imipramine-G from 44 individual donor HLMs were determined by Spearman's rank method. When *P* value was less than 0.05, the correlations were considered statistically significant.

Results

Analysis of AP-G in UGTs

UGT1A4 (71%), 1A3 (19%), and 1A8 (10%) are responsible for glucuronidation of aprepitant and were therefore assessed in this study (Figure 1). A glucuronide peak eluted at 6.1 min with the MRM transition pair [MH^+] = (711.2/179.2) which follows a previously determined structure transformation (Huskey et al., 2004) and new mass. AP-G was not detected following incubation with UGT1A1, UGT1A6, UGT1A7, UGT1A9, UGT1A10, UGT2B4, UGT2B7, UGT2B10, UGT2B15, UGT2B17, and control Supersomes.

The velocities at 5 μM were 44.1 ± 0.7 [CV=15.9%] and 124.6 ± 6.4 [5.1%] (fmol/min/mg protein) for UGT1A3 and UGT1A4, respectively. The velocities at 250 μM were 717.3 ± 18.6 [2.6%], 2,710 ± 157.2 [5.8%], and 391 ± 10.6 [2.7%] (fmol/min/mg protein) for UGT1A3, UGT1A4, and UGT1A8 respectively. HLMs yielded a velocity of 177.2 ± 6.3 [3.6%] (fmol/min/mg protein) and 2,470 ± 10 [0.4%] (fmol/min/mg protein) for 5 μM and 250 μM respectively. HIMs yielded a velocity of 278.3 ± 1.9 [0.7%] (fmol/min/mg protein) at 250 μM. No detectable glucuronide was formed at 5 μM (Figure 1).

Analysis of AP-G in HLMs and HIMs

AP-G was detected following aprepitant incubation with HLMs and HIMs in the presence of UDPGA. This product was absent when the incubation mixture was missing UDPGA, substrate, or protein (data not shown).

Kinetic Studies in HLMs, HIMs, and UGTs

We investigated the kinetics of aprepitant glucuronidation in pooled HLMs, HIMs and relevant UGTs. For pooled HLMs, the velocity curve exhibited a biphasic shape (Figure 2A inset) indicating a low and high affinity component, but data for K_m is not shown due to extrapolation and subsequent high error. For HIMs, the velocity curve followed Michaelis-Menten kinetics (Figure 2B inset). The velocity curves for UGT1A3 and UGT1A4 followed typical Michaelis-Menten kinetics (Figures 2C and 2D inset), while UGT1A8-catalyzed aprepitant glucuronidation followed sigmoidal kinetics with substrate activation which manifests as a curvilinear Eadie-Hofstee plot (Figure 2E inset). K_m or S_{50} values are shown in Table 1.

Inhibition of Aprepitant Glucuronidation

Since our UGT screening data showed that glucuronidation occurs only by UGT1A3, 1A4 and 1A8, we performed inhibition studies of these enzymes along with HLMs and HIMs with highly specific inhibitors (Table 2). For inhibition experiments involving UGTs with clinically relevant aprepitant concentrations (5 μM), we observed complete inhibition of aprepitant glucuronidation by UGT1A3 and UGT1A4. Glucuronidation by UGT1A8 was not observed at this concentration. At the respective K_ms, there was high inhibition of UGT1A3, UGT1A4 and UGT1A8. For inhibition experiments involving HLMs, using aprepitant at 5 μM and at the K_ms, we observed high inhibition using hecogenin and minor inhibition (<25%) using sulfinpyrazone. Inhibition of glucuronidation by HIMs could not be investigated using 5 μM aprepitant as glucuronide was not formed. Glucuronidation by HIMs was completely inhibited at the K_m for UGT1A8 (197 μM).

Correlation Analyses

The overall glucuronidation activity of aprepitant in microsomes from 44 livers varied approximately 2-fold ranging from 366 to 852 fmol/min/mg protein. The mean value (±S.D.) and coefficient of variation were 552.8 ± 145.7 [26.4%] (fmol/min/mg protein). Rates of aprepitant glucuronidation were best correlated with anastrazole (Figure 3A) and imipramine glucuronidation (Figure 3B) ($r_s = 0.77$, $P < 0.0001$ for both substrates). A significant correlation was also observed with thyroxine glucuronidation ($r_s = 0.58$, $P < 0.0001$) (Figure 3C).

Inhibition by Aprepitant of UGTs

Inhibition of UGTs was tested by aprepitant with imipramine (a substrate for UGT1A4) and 4-MU (a substrate for all isoforms except UGT1A4 and UGT2B10) (Uchaipichat et al., 2004). At 1 μM, aprepitant was found to inhibit UGT2B7 glucuronidation by approximately 17%. Inhibition of other UGTs was <10%. At 10 μM, aprepitant showed the highest inhibitory effect (70%) on UGT2B7 glucuronidation followed by UGT1A6 (19%), UGT1A4 (18%), UGT1A7 (17%) and UGT2B17 (10%).

Inhibition by Aprepitant of 4-MU-G, M-6-G, and AZT-G Formation Rate by UGT2B7

The representative Lineweaver-Burke and Dixon plots are shown for 4-MU-G inhibition (Figure 4A, 4B), M-6-G inhibition (Figure 4C, 4D), and AZT-G inhibition (Figure 4E, 4F).

Data were best fitted to a competitive inhibition model for 4-MU and AZT glucuronidation, while morphine glucuronidation exhibited a noncompetitive model. K_i values for inhibition by aprepitant were 7.4 μM for 4-MU, 16.3 μM for morphine, and 6.7 μM for AZT.

Inhibition by Aprepitant of M-6-G Formation Rate by UGT2B7 in pHs of 6.5 and 7.5

The representative Dixon plots are shown for K_i determination in a pH buffer of 6.5 (Figure 5A), and pH buffer of 7.5 (Figure 5B). The K_i for aprepitant was determined to be 15.1 μM and 15.5 μM for pH 6.5 and pH 7.5 respectively.

Discussion

The goal of this study was to assess the major UGT isoforms involved in the glucuronidation of aprepitant *in vitro*. Moreover, we showed that aprepitant is a moderate inhibitor of intestinal UGT2B7 and can potentially affect the clearance of orally co-administered drugs that are eliminated via this pathway. These findings provide the first demonstration of aprepitant glucuronidation in human liver and intestine and further allude to potential drug interactions associated with concomitant use with aprepitant.

The major UGT isoforms involved in aprepitant metabolism are UGT1A4 and UGT1A3. The characterization of involvement of these enzymes in the metabolism of aprepitant was confirmed by performing inhibition studies (Table 2). When selectively inhibiting UGT1A4 in HLM, we demonstrated 81% inhibition. When selectively inhibiting UGT1A3 in HLM, glucuronidation was only suppressed by 22%. These data are in agreement with our screening results (Figure 1). Taken together, we can conclude that UGT1A4 is the primary isoform responsible for the glucuronidation of aprepitant with minor contribution from UGT1A3.

In human liver microsomes, aprepitant primarily undergoes *N*- and *O*-dealkylation via cytochrome P450 system, with *N*-dealkylation primarily from CYP3A4 and *O*-dealkylation from CYP1A2, CYP2C19, and CYP3A4 (Sanchez et al., 2004). A previous study in rats and dogs showed aprepitant metabolism yielded twelve oxidative metabolites and one primary glucuronide metabolite (Huskey et al., 2003). This study further noted four potential structures (regioisomeric) for AP-G, but was unable to differentiate between *O*- and *N*-glucuronide formation. While our studies confirmed a glucuronide was formed in humans *in vitro*, we were unable to delineate which of the four possible glucuronides were formed based on mass spectroscopic data alone. However, we believe that this is an *N*-glucuronide since UGT1A4 is the primary catalyzer and it has been shown that UGT1A4 preferentially catalyzes the conjugation of tertiary amines to quaternary *N*-glucuronides (Green et al., 1995).

In order to assess the properties of enzymatic activity for the glucuronidation of aprepitant in HLMs, K_m determination would have been used. However, we were unable to determine this because V_{max} was not obtained due to the poor solubility of aprepitant (our determined aqueous solubility was ~250 μM), and K_m estimates would be unreliable. The different K_m value for HIMs compared to UGT1A8 may be attributed to the fact that HIMs express

multiple enzymes (including UGT1A3 and 1A4 in addition to 1A8; Court et al 2012, Nakamura et al., 2008), and UGT1A8 has the lowest affinity with the substrate.

While the discovery of aprepitant glucuronidation in HLMs is novel, the overall relative glucuronidation rates that we observed are low when compared to oxidative metabolism rates. A group studying phase I metabolism in HLMs found a significantly higher conversion rate for aprepitant (Sanchez et al., 2004). Even though it appears that the main route for aprepitant elimination is phase I metabolism via CYP3A4, the relevance of aprepitant as an inhibitor of UGT2B7 remains a significant finding and warrants additional study.

We evaluated aprepitant as an inhibitor of intestinal UGT2B7 by calculating the clinical concentration of aprepitant that passes from the lumen of the gut into the enterocyte (equation 1). Since the intestinal absorption of orally administered drugs *in vivo* is primarily passive diffusion driven by the concentration of the drug in the lumen (Lennernas H., 2007), we calculated the luminal concentration of aprepitant to be between 300 μM (40 mg oral capsule) and 936 μM (125 mg oral capsule). With a mean absolute oral bioavailability of 60–65% (Merck 2003), and the length of time that it would take for a capsule to traverse the small bowel (~7 hrs.)(Evans et al., 1988), we believe the concentration of aprepitant is high enough and the time of action is long enough to achieve moderate inhibition of UGT2B7 in enterocytes during first pass intestinal metabolism.

We also investigated aprepitant as an inhibitor of UGT2B7 activity at the pH range in the small intestine as this is where absorption and first-pass metabolism would occur. A pH range of 6.5 (in the duodenum) to 7.5 (in the distal small intestine) was reported by (Fallingborg, 1999; Evans et al., 1988). Our data suggests that this pH range has no effect on the enzyme catalyzed reaction rate.

There are several known drugs that are metabolized primarily by UGT2B7. Two notable drugs that have the potential to be co-administered with aprepitant are morphine and zidovudine (AZT). The prodrug morphine is exclusively catalyzed by UGT2B7 to form morphine-3-glucuronide and M-6-G (a more potent agonist than morphine itself) (Abbott et al, 1988; Holthe et al., 2003; Sawyer et al., 2003). We have shown herein that aprepitant acts as a moderate inhibitor on morphine glucuronidation by UGT2B7 (Figure 4). Additionally, this enzyme does not metabolize aprepitant (Figure 1). These findings suggest that aprepitant binds to an allosteric site causing noncompetitive inhibition of UGT2B7 and can potentially decrease the production of M-6-G. This would have clinical implications as patients could receive less therapeutic benefit following a given dose of morphine. Further study of this potential drug-drug interaction is warranted *in vivo*.

AZT is extensively used for the treatment of HIV-infected individuals and may also be co-administered with aprepitant since it has been shown that aprepitant significantly enhances the anti-HIV activity of concomitant antiretrovirals (such as AZT) in macrophages *in vitro* (Wang et al., 2007). AZT glucuronidation is primarily (60–70%) catalyzed by UGT2B7 (Veal et al., 1995; Barbier et al., 2000). Aprepitant acts as a moderate inhibitor of AZT glucuronidation by UGT2B7 with an apparent K_i of 6.7 μM (assessed herein). Consequently, aprepitant could potentially inhibit the first pass intestinal metabolism of AZT. Additionally,

there is potential for inhibition of UGT2B7 metabolism in hepatic tissue since the systemic circulation of aprepitant in patients is approximately 5 μM (Lasseter et al., 2007; Takahashi et al., 2011). However, as with many drugs, aprepitant is highly protein bound (~95%), and further studies are necessary to investigate this effect *in vivo*.

Conclusions

The results presented in this paper further characterize the metabolism of aprepitant. It is known that aprepitant is metabolized by CYP1A2, CYP2C19 and CYP3A4 and is also a moderate inhibitor of CYP3A4 (Sanchez et al., 2004). It has now been shown to undergo glucuronidation primarily by UGT1A4, and also moderately inhibits UGT2B7. Based on our results, we hypothesize that patients receiving morphine or AZT may demonstrate increased bioavailability if administered with aprepitant.

References

Abbott FV, Palmour RA. Morphine-6-glucuronide: Analgesic effects and receptor binding profile in rats. Life Sciences. 1988; 43:1685–1695. [PubMed: 2848167]

Barbier O, Turgeon D, Girard C, Green MD, Tephly TR, Hum DW, Belanger A. 3'-Azido-3'-Deoxythimidine (AZT) is glucuronidated by human UDP-glucuronosyltransferase 2B7 (UGT2B7). Drug Metab Dispos. 2000; 28:497–502. [PubMed: 10772627]

Chang, R. Physical Chemistry for the Biosciences (University Science books). Herndon, VA: 2005. Enzyme Inhibition; p. 377-385.

Court MH, Krishnaswamy S, Hao Q, Duan SX, Patten CJ, Von Moltke LL, Greenblatt DJ. Evaluation of 3'-Azido-3'-Deoxythymidine, morphine, and codeine as probe substrates for UDP-glucuronosyltransferase 2B7 (UGT2B7) in human liver microsomes: specificity and influence of the UGT2B7*2 polymorphism. Drug Metab Dispos. 2003; 31:1125–1133. [PubMed: 12920168]

Court MH, Zhang X, Ding X, Yee KK, Hesse LM, Finel M. Quantitative distribution of mRNAs encoding the 19 human UDP-glucuronosyltransferase enzymes in 26 adult and 3 fetal tissues. Xenobiotica. 2012; 42:266–277. [PubMed: 21995321]

Dong RH, Fang ZZ, Zhu LL, Liang SC, Ge GB, Yang L, Liu ZY. Investigation of UDP-glucuronosyltransferases (UGTs) inhibitory properties of carvacrol. Phytother Res. 2012; 26:86–90. [PubMed: 21544887]

Evans DF, Pye G, Bramley R, Clark AG, Dyson TJ, Hardcastle JD. Measurement of gastrointestinal pH profiles in normal ambulant subjects. Gut. 1988; 29:1035–1041. [PubMed: 3410329]

Fallingborg J. Intraluminal pH of the human gastrointestinal tract. Danish Medical Bulletin. 1999; 46:183–195. [PubMed: 10421978]

Green MD, Bishop WP, Tephly TR. Expressed human UGT1.4 protein catalyzes the formation of quaternary ammonium-linked glucuronides. Drug Metab Dispos. 1995; 23:299–302. [PubMed: 7628292]

Holthe M, Rakvag TN, Klepstad P, Idle JR, Kaasa S, Krokan HE, Skorpen F. Sequence variations in the UDP-glucuronosyltransferase 2B7 (UGT2B7) gene: identification of 10 novel single nucleotide polymorphisms (SNPs) and analysis of their relevance to morphine glucuronidation in cancer patients. Pharmacogenomics J. 2003; 3:17–26. [PubMed: 12629580]

Huang SM, Zhang L. Draft Guidance/Guidance for Industry. Drug interaction studies-study design, data analysis, implications for dosing, and labeling recommendations. Center for Drug Evaluation and Research (CDER). 2012

Huskey SW, Dean BJ, Doss GA, Wang Z, Hop CECA, Anari R, Finke PE, Robichaud AJ, Zhang M, Wang B, Strauss JR, Cunningham PK, Feeney WP, Franklin RB, Baillie TA, Chiu S-HL. The metabolic disposition of aprepitant, A substance p receptor antagonist, in rats and dogs. Drug Metab Dispos. 2004; 32:246–258. [PubMed: 14744948]

Hutzler JM, Tracy TS. Atypical kinetic profiles in drug metabolism reactions. Drug Metab Dispos. 2002; 30:355–362. [PubMed: 11901086]

Innocenti F, Iyer L, Ramírez J, Green MD, Ratain MJ. Epirubicin glucuronidation is catalyzed by human UDP-glucuronosyltransferase 2B7. Drug Metab Dispos. 2001; 29:686–692. [PubMed: 11302935]

Kaivosaari S, Finel M, Koskinen M. N-glucuronidation of drugs and other xenobiotics by human and animal UDP-glucuronosyltransferases. Xenobiotica. 2011; 41:652–669. [PubMed: 21434773]

Kamdem LK, Liu Y, Stearns V, Kadlubar SA, Ramirez J, Jeter S, Shahverdi K, Ward BA, Ogvurn E, Ratain MJ, Flockhart DA, Desta Z. *In vitro* and *in vivo* oxidative metabolism and glucuronidation of anastrozole. Br J Clin Pharmacol. 2010; 70:854–869. [PubMed: 21175441]

King CD, Rios MD, Green MD, Tephly TR. UDP-Glucuronosyltranferases. Curr Drug Metab. 2000; 1:143–161. [PubMed: 11465080]

Lasseter KC, Gambale J, Jin B, Bergman A, Constanzer M, Dru J, Han TH, Majumdar A, Evans JK, Murphy GE. Tolerability of fosaprepitant and bioequivalency to aprepitant in healthy subjects. J Clin Pharmacol. 2007; 47:834–840. [PubMed: 17525168]

Lennernas H. Intestinal permeability and its relevance for absorption and elimination. Xenobiotica. 2007; 37:1015–1051. [PubMed: 17968735]

Liu Y, Ramirez J, House L, Ratain MJ. Comparison of the drug-drug interactions potential of erlotinib and gefitinib via inhibition of UDP-glucuronosyltransferases. Drug Metab Dispos. 2010; 38:32–39. [PubMed: 19850672]

Merck Sharp & Dohme Corp., a subsidiary of Merck & Co., Inc.. Emend [package insert]. Whitehouse Station, NJ. 9985512: 2003.

Nakajima M, Tanaka E, Kobayashi T, Ohashi N, Kume T, Yokoi T. Imipramine N-glucuronidation in human liver microsomes: biphasic kinetics and characterization of UDP-glucuronosyltransferase isoforms. Drug Metab Dispos. 2002; 30:636–642. [PubMed: 12019188]

Nakamura A, Nakajima M, Yamanaka H, Fujiwara R, Yokoi T. Expression of UGT1A and UGT2B mRNA in human normal tissues and various cell lines. Drug Metab Dispos. 2008; 36:1461–1464. [PubMed: 18480185]

Olver IN. Aprepitant in antiemetic combinations to prevent chemotherapy-induced nausea and vomiting. Int J Clin Pract. 2004; 58:201–206. [PubMed: 15055869]

Sanchez RI, Wang RW, Newton DJ, Bakhtiar R, Lu P, Lee Chiu S-H, Evans DC, Huskey SW. Cytochrome P450 is the major enzyme involved in the metabolism of the substance p receptor antagonist aprepitant. Drug Metab Dispos. 2004; 32:1287–1292. [PubMed: 15304427]

Sawyer MB, Innocenti F, Das S, Cheng C, Ramirez J, Pantle-Fisher FH, Wright C, Badner J, Pei D, Boyett JM, Cook E, Ratain MJ. A pharmacogenetic study of uridine diphosphate-glucurosyltransferase 2B7 in patients receiving morphine. Clin Pharmacol Ther. 2003; 73:566–574. [PubMed: 12811366]

Shadle CR, Lee Y, Majumdar AK, Petty KJ, Gargano C, Bradstreet TE, Evans JK, Blum RA. Evaluation of potential inductive effects of aprepitant on cytochrome P450 3A4 and 2C9 activity. J Clin Pharmacol. 2004; 44:215–223. [PubMed: 14973304]

Takahashi T, Nakamura Y, Tsuya A, Murakami H, Endo M, Yamamoto N. Pharmacokinetics of aprepitant and dexamethasone after administration of chemotherapeutic agents and effects of plasma substance P concentration on chemotherapy-induced nausea and vomiting in Japanese cancer patients. Cancer Chemother Pharmacol. 2011; 68:653–659. [PubMed: 21125277]

Uchaipichat V, Mackenzie PI, Guo XH, Gardener-Stephen D, Galetin A, Houston JB, Miners JO. Human UDP-glucuronosyltransferases: isoform selectivity and kinetics of 4-methylumbelliferone and 1-naphthol glucuronidation, effects of organic solvents, and inhibition by diclofenac and probenecid. Drug Metab Dispos. 2004; 32:413–423. [PubMed: 15039294]

Uchaipichat V, Mackenzie PI, Elliot DJ, Miners JO. Selectivity of substrate (trifluoperazine) and inhibitor (amytriptylene, androsterone, canrenoic acid, hecogenin, phenylbutazone, quinidine, quinine, and sulfinpyrazone) “probes” for human UDP-glucurosyltransferases. Drug Metab Dispos. 2006; 34:449–456. [PubMed: 16381668]

Veal GJ, Back DJ. Metabolism of Zidovudine. Gen Pharmac. 1995; 26:1469–1475.

Walsky RL, Bauman JN, Bourcier K, Giddens G, Lapham K, Negahban A, Ryder F, Obach RS, Hyland R, Goosen T. Optimized assays for human UDP-glucuronosyltransferase (UGT) activities: altered alamethicin concentration and utility to screen for UGT inhibitors. Drug Metab Dispos. 2012; 40:1051–1065. [PubMed: 22357286]

Wang X, Douglas SD, Lai JP, Tulue F, Tebas P, Ho WZ. Neurokinin-1 receptor antagonist (aprepitant) inhibits drug-resistant HIV-1 infection of macrophages in vitro. J Neuroimmune Pharmacol. 2007; 2:42–48. [PubMed: 18040825]

Wu D, Paul DJ, Zhao X, Douglas SD, Barrett JS. A sensitive and rapid liquid chromatography-tandem mass spectrometry method for the quantification of the novel neurokinin-1R-antagonist aprepitant in rhesus macaque plasma, and cerebral spinal fluid, and human plasma with application in translational neuroAIDS research. J Pharm Biomed Anal. 2009; 49:739–745. [PubMed: 19167182]

Yoder Graber AL, Ramirez J, Innocenti F, Ratain MJ. UGT1A1*28 genotype affects the *in vitro* glucuronidation of thyroxine in human livers. Pharmacogenet Genomics. 2007; 17:619–627. [PubMed: 17622938]

Zhang L, Zhang Y, Stong JM, Reynolds KS, Huang S. A regulatory viewpoint on transporter-based drug interactions. Xenobiotica. 2008; 38:709–724. [PubMed: 18668428]

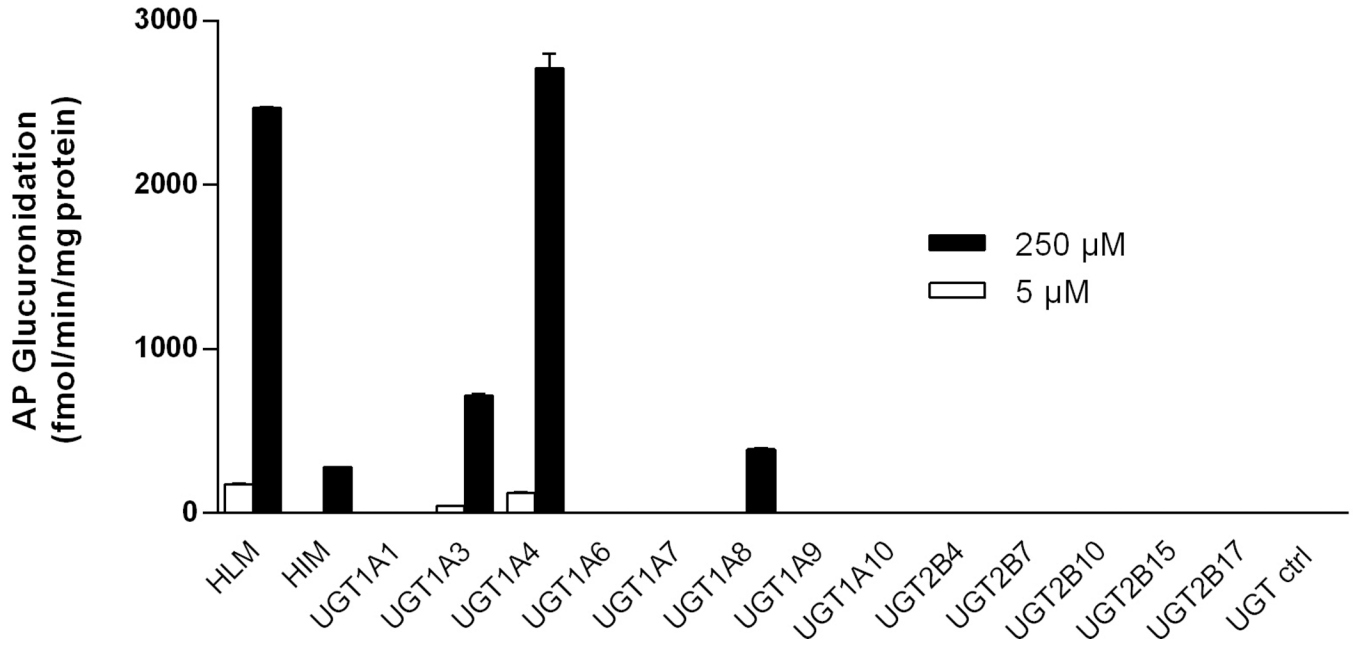

Figure 1.

Screening of HLM, HIM and Supersomes expressing functional human UDP-glucuronosyltransferases (UGTs) for AP-G formation. Incubations were performed with 0.5 mg/ml of microsomal protein and 5 µM or 250 µM aprepitant for 60 min at 37°C. Data represent means of triplicate determination ± SE.

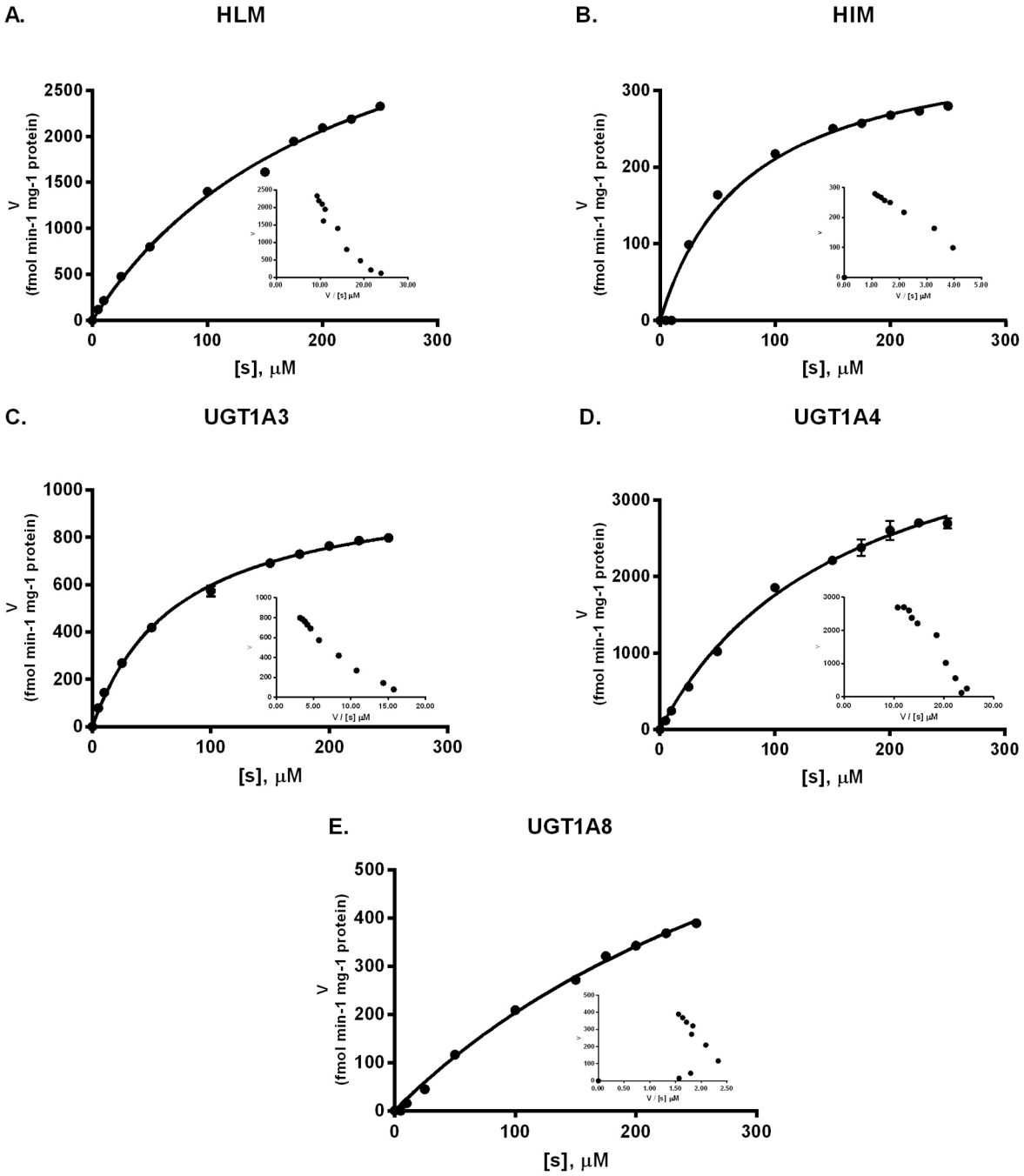

Figure 2.

Enzyme kinetics of aprepitant glucuronidation in (A) human liver microsomes (HLM), (B) human intestinal microsomes (HIM), (C) UGT1A3, (D) UGT1A4, and (E) UGT1A8. Eadie-Hofstee plots are inset. Enzyme kinetic parameters for HIM, UGT1A3, UGT1A4 and UGT1A8 are shown in Table 1. K_m parameters for HLM are not shown. Data represent means of triplicate determination ± SE.

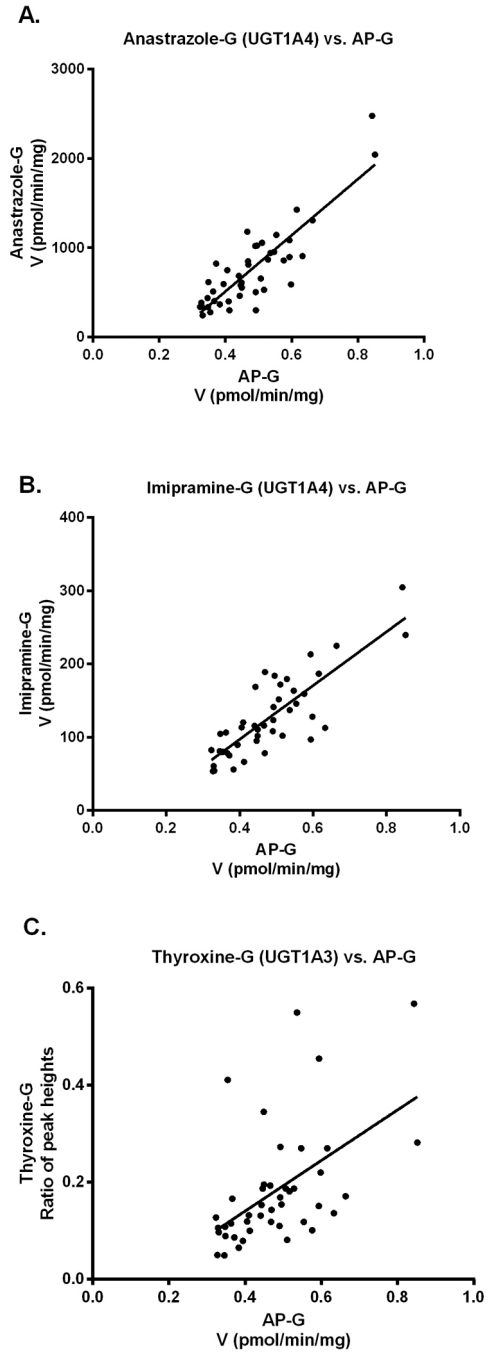

Figure 3.

Correlation of aprepitant glucuronidation with (A) anastrazole, (B) imipramine, and (C) thyroxine glucuronidation. Incubations with aprepitant (30 μM) were performed with 0.5 mg/ml of human liver microsomes (HLM) for 60 min at 37°C. Anastrazole and imipramine glucuronidation are expressed as velocity (pmol/min/mg) of protein. Thyroxine glucuronidation is expressed as the ratio of thyroxine glucuronide peak heights to the internal standard. Aprepitant glucuronidation data represent means of duplicate determination.

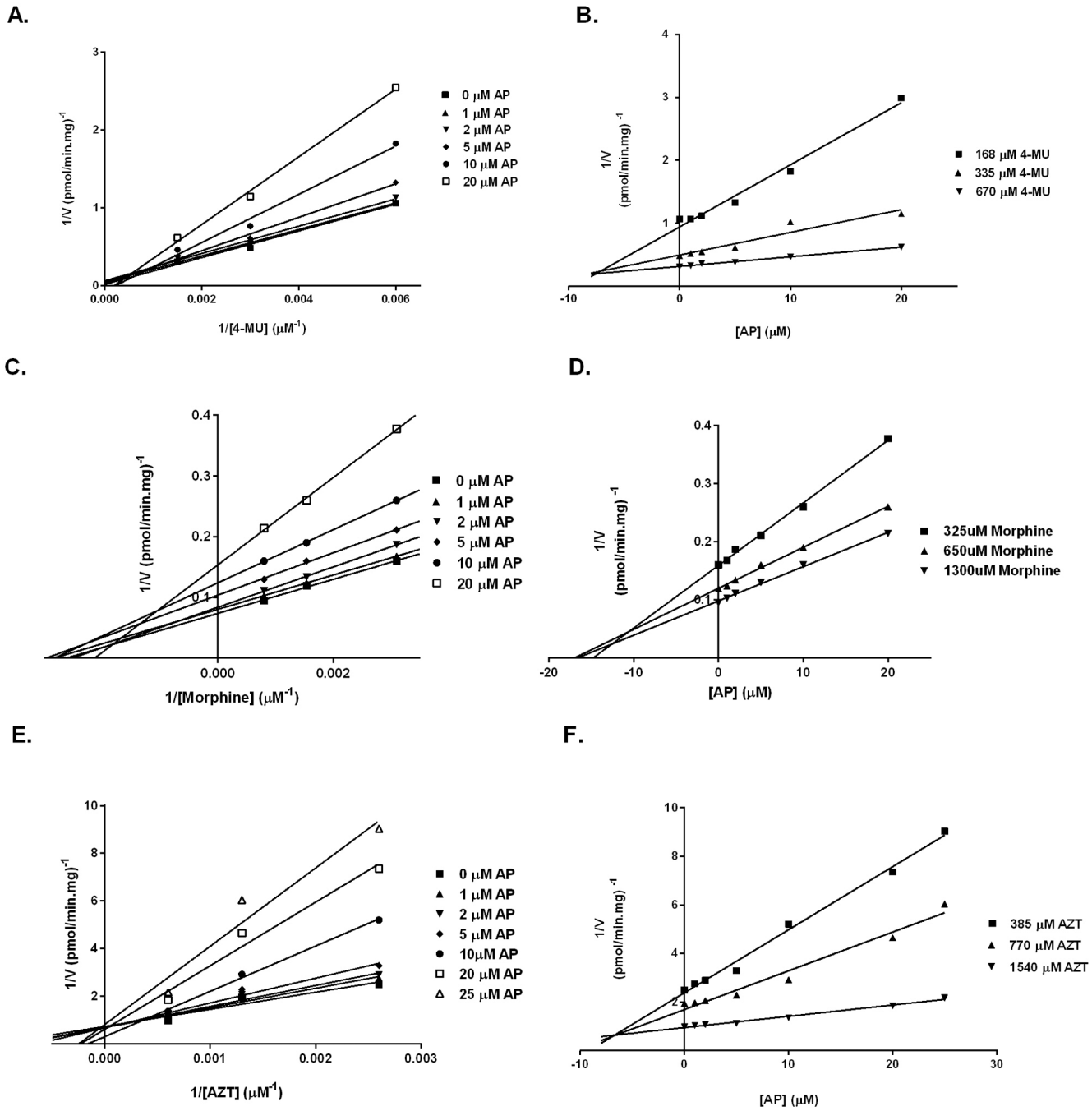

Figure 4.

Representative Lineweaver-Burk and Dixon plots for the inhibition of UGT2B7-catalyzed 4-MU glucuronidation (A, B), morphine glucuronidation (C, D), and AZT glucuronidation (E, F) by aprepitant. Data represent means of triplicate determination.

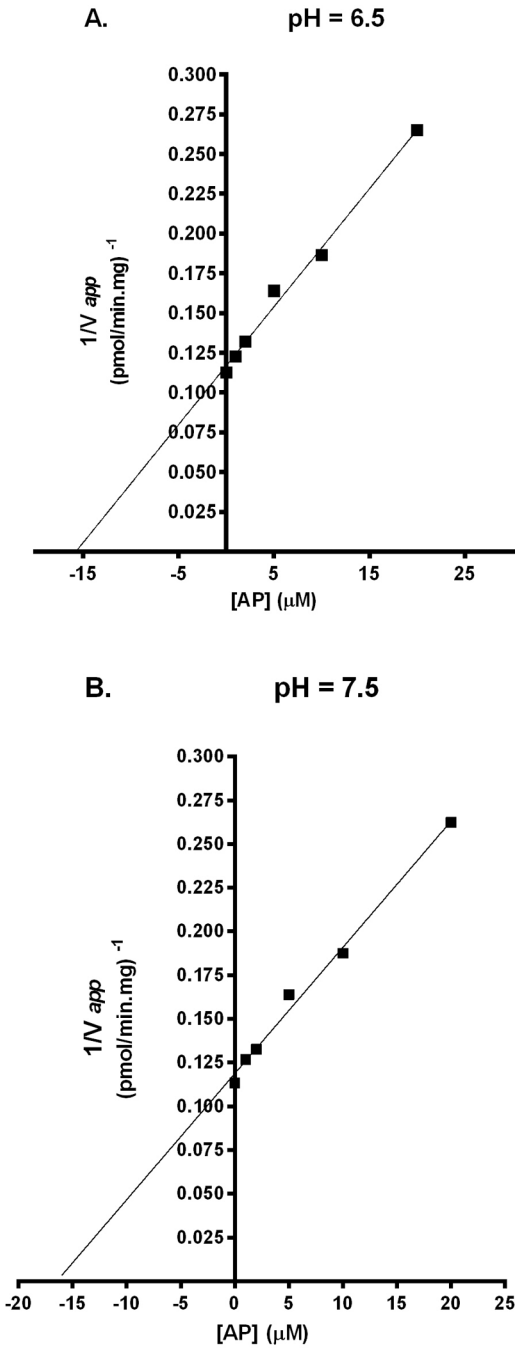

Figure 5.

Representative Dixon plots for aprepitant inhibition of morphine glucuronidation at K_m = 650 μM. The K_i was 15.1 μM for pH 6.5 (Figure 5A) and 15.5 μM for pH 7.5 (Figure 5B). Data represent means of triplicate determination.

Table 1

Kinetic parameters for aprepitant glucuronidation in HIMs and recombinant UGT enzymes.

Enzyme	Kinetics model	K_m or S_{50}	V_{max}	CL_{int}	*n*
		(μM)	**(fmol/min/mg protein)**	**(μl/min/μg protein)**	
HIM	Michaelis-Menten	63 ± 5	352 ± 8	5.6	N.A.
UGT1A3	Michaelis-Menten	69 ± 2	1,030 ± 16	15	N.A.
UGT1A4	Michaelis-Menten	162 ± 16	4,588 ± 222	28	N.A.
UGT1A8	Hill	197 ± 28	683 ± 69	3.5	1.2 ± 0.1

K_m, apparent substrate concentration at half-maximal velocity; S_{50}, apparent substrate concentration at half-maximal velocity for substrates exhibiting atypical sigmoidal kinetics; V_{max}, maximal velocity; CL_{int}, intrinsic clearance; *n*, Hill coefficient; N.A., not applicable. Values are expressed as Means ± SE.

Table 2

Percent inhibition of aprepitant glucuronidation with UGT specific inhibitors.

Enzyme	Inhibitor[c]	Aprepitant (5 μM)	Aprepitant (K_m)[b]
HIM	diclofenac	N.A.[a]	100%
UGT1A8	diclofenac	N.A.[a]	66.7%
HLM	sulfinpyrazone	22.2%	22.1%
UGT1A3	sulfinpyrazone	100 %	100%
HLM	hecogenin	100%	80.8%
UGT1A4	hecogenin	100%	83.9%

N.A., not applicable.

[a] At 5 μM, HIMs and UGT1A8 showed no activity.

[b] The respective K_ms for aprepitant were 197 μM for UGT1A8 (the same concentration was used for HIMs); 69 μM for UGT1A3 (the same concentration was used for HLMs), 162 μM for UGT1A4 (the same concentration was used for HLMs).

[c] Inhibitor concentrations were as follows: 500 μM diclofenac, 1000 μM sulfinpyrazone, and 200 μM hecogenin.